

# LATEST ACHIEVEMENTS ON RECONFIGURABLE REFLECTOR ANTENNAS MODELLING

K. Pontoppidan<sup>(1)</sup>, C. Cappellin<sup>(1)</sup>, N.C. Jessen<sup>(2)</sup>, H.U. Nørgaard-Nielsen<sup>(2)</sup>

<sup>(1)</sup> TICRA, Læderstræde 34, DK-1201 Copenhagen K, Denmark, Email: ticra@ticra.com

<sup>(2)</sup> DTU Space, Juliane Maries Vej 30, DK-2100 Copenhagen Ø, Denmark, Email: nej@space.dtu.dk

## ABSTRACT

This paper describes various aspects of a reconfigurable reflector antenna for future space applications. The reflector surface consists of an RF net made by thin interwoven piano wires. This net provides the necessary reflectivity at Ku-band frequencies. The RF net is very soft and it is therefore supported by a thicker net of the same construction. The reflector is shaped by means of a number of actuators across the surface. The paper presents accurate mechanical Finite Element Method calculations to validate the fast numerical method developed in previous studies for the optimisation of the surface shape for different antenna coverage regions.

## 1 INTRODUCTION

A number of different reconfigurable reflector concepts have been studied in the past. The first attempts used a tricot mesh suspended over a fixed rim and with a number of actuators distributed over the surface. This approach gives rise to heavy pillowing effects and therefore a tricot mesh attached to flexible wires was later investigated. The next step in this evolution was to skip the tricot mesh and use only a net of interwoven flexible wires [1]. The present paper is a further development of this approach. Recently an investigation has started at ESA where a deformable reflector made of CFRS (Carbon Fibre Reinforced Silicone) is used [2].

The reconfigurable reflector concept described in [1] is a net of interwoven flexible wires perpendicular to each other and supported by a finite number of actuators. Such a surface remains smooth everywhere, also at the control points, and it does not generate singularities and wrinkles. In addition, this reflector does not need any support along the rim. A mathematical model of the surface was found based on a linear approximation of the wire deformations, and an efficient optimization algorithm was developed to determine the best control point positions for a given set of antenna coverage regions.

The performances and numerous advantages achieved by a shaped reflector equipped with a reconfigurable

surface of this type have been presented previously, [3] and [4]. A demonstrator model 30 cm in diameter was also built using interwoven piano wires of diameter 0.3 mm, equidistantly spaced by 10 mm and supported by 9 actuators. A photo of this model is shown in Figure 1.

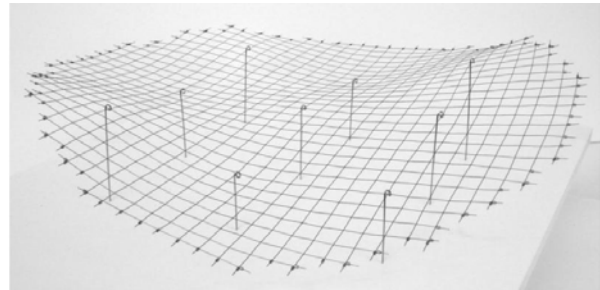


Figure 1 The TICRA Lab Model. The diameter is 30 cm, the piano wires have a diameter of 0.3 mm and the distance between the wires is 10 mm.

To fully prove the feasibility of the proposed reconfigurable surface for Ku-band applications, a detailed Finite Element Method (FEM) analysis is necessary. Such an analysis should validate the accuracy of the surface shape and the mechanical properties computed previously by the fast mathematical model. A proper wire spacing ensuring reflectivity at Ku-band should finally be defined.

The purpose of the present paper is to introduce an improved reconfigurable reflector technology able to provide reflectivity and reconfigurability at Ku-band, and to show the results of a thorough FEM analysis of such a surface. In particular, we will illustrate how the use of two nets, a coarse one supporting a fine one, can provide the necessary rigidity to be handled on ground and at the same time the necessary reflectivity and elasticity. We will also show that the surface computed so far by the linear approximation perfectly matches the surface obtained by a linear FEM analysis.

Possible Passive InterModulation (PIM) problems are not considered in this paper.

The paper is organized as follows: In Section 2 the improved reconfigurable reflector concept is described, with emphasis on reflectivity properties, practical realization and a guideline for proper dimensioning. Section 3 deals with the computation of the surface shape, showing FEM analysis results with linear and non-linear deformations, and a comparison with previous computations, while Section 5 describes important mechanical properties of the interwoven wire net. Conclusions are finally drawn in Section 6.

## 2 PROPOSED RECONFIGURABLE REFLECTOR CONCEPT

Though the reflector model in Figure 1 shows excellent reconfiguration properties, it suffers from a main weakness, namely the practical realization of a reconfigurable interwoven wire surface able to work in Ku-band. It is evident that a net with spacing of 10 mm cannot provide the necessary reflection at a typical Ku-band frequency, i.e. 15 GHz corresponding to a wavelength of 20 mm, since at this frequency the necessary spacing between the wires cannot exceed about 1 mm. A reduction of the spacing by a factor 10 requires a corresponding reduction of the wire diameter to 0.03 mm, in order to maintain the elastic properties of the net. While this could work in space, the gravity on the Earth will make such a model impossible to build and test.

Based on the above observations the proposed reconfigurable reflector will contain the following elements:

- Support net, typically 0.3 mm piano wires with 10 mm spacing
- RF net, typically 0.03 mm piano wires with 1 mm spacing
- Actuators mounted on a rear shell and attached to control points on the support net.

The number of wire intersections in the support net for a realistic reflector can be very large, typically 10-20,000. A few of these intersection points, typically 50-100, are selected as control points for the reconfiguration and to which the actuators are attached.

It is necessary to distinguish between three types of connections between the actuators and the control points. We assume that the support net is located with its centre at the origin of an  $xy$ -coordinate system (see Figure 3):

1. The actuator at the origin,  $(x, y) = (0, 0)$ : the connection is stiff such that the control point can only move in the  $z$ -direction.
2. One or more of the actuators on the  $x$ -axis: the connection has a hinge such that it can follow movements of the control points in

the  $x$ -direction. Similarly for actuators on the  $y$ -axis.

3. All other actuators: the connection is free to allow movements of the control points on the net along both  $x$  and  $y$ .

The above requirements are sufficient to specify the reflector completely.

In order to illustrate the feasibility of the concept the model in Figure 1 has been supplied with an RF net as shown on the photo in Figure 2. In this case the RF net is a molybdenum net with 0.1 mm wires and a spacing of 0.85 mm. The figure shows that the RF net follows the support net in all details.

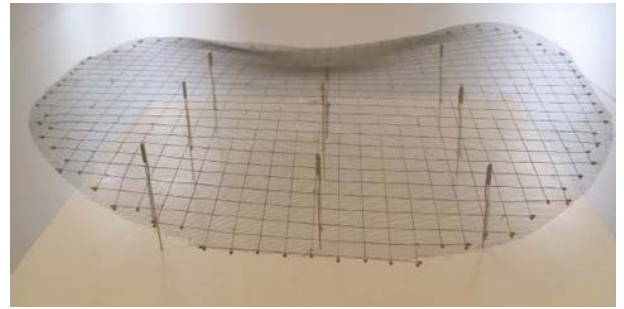


Figure 2 The model in Figure 1 with the RF net attached.

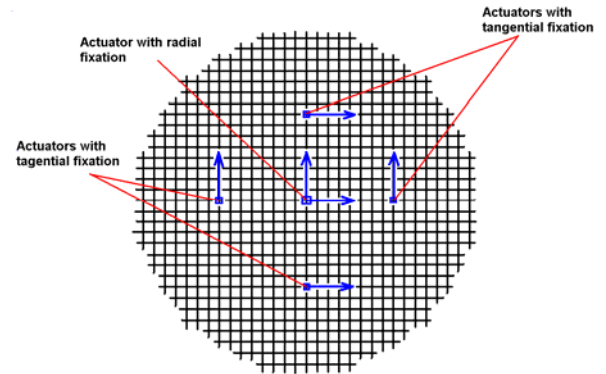


Figure 3 Fixation of the support net.

### 2.1 Reflection properties of the RF net

The complex amplitude reflection coefficient,  $R$ , for a square wire net at normal incidence is given by [5]

$$R = \frac{1}{1 + j \frac{2s}{\lambda} \ln \frac{s}{\pi d}}$$

where  $s$  is the spacing between the wires,  $\lambda$  is the wavelength at the operating frequency and  $d$  is the

diameter of the wires. For normal incidence the reflection coefficient is independent of the polarisation. For non-normal incidence the reflection coefficient decreases slightly with increasing angle of incidence if the field is polarised in the plane of incidence and it increases slightly for the orthogonal polarisation.

As an example, for  $s = 1$  mm,  $\lambda = 20$  mm (15 GHz) and  $d = 0.03$  mm the power reflection is 0.95 (-22 dB).

## 2.2 Principles for dimensioning

In a realistic case the available reflector diameter and the operating frequency will be given. The requirements to reconfigurability of the antenna coverage zones will determine the number of control points and the distance between them, see [4]. Hence, the input parameters for the mechanical reflector design are:

- The frequency, for example 15 GHz corresponding to a wavelength of  $\lambda = 20$  mm.
- Reflector diameter, for example 1.5 m.
- The number of control points and the distance  $C$  between them, for example  $C = 10$  cm.

With these inputs the wire net parameters can be determined as follows:

- Select the support wire spacing,  $S$ , not larger than  $S = C / 4$ . This will ensure that the support net is able to provide the required flexibility of the surface
- Select the support wire diameter,  $D$ , as small as possible but large enough to maintain a surface deformation due to gravity (from both support and RF net) within  $\lambda/100$ .
- Check that  $D < 0.03S$  (piano wire). This will ensure that deformations are well within the elastic limit.
- Select RF wire spacing,  $s$ , such that  $s < \lambda / 20$  to ensure sufficient reflectivity.
- Select the RF net material and wire diameter.
- Check that the sagging due to gravity of the RF net is within 0.1 mm. It can be assumed that the RF net is attached at the four corners of the support net element cell.

## 3 CALCULATION OF THE SURFACE SHAPE

In this section we will study how to accurately compute the shape of a surface given by a net of interwoven wires. We will concentrate on the 30 cm x 30 cm model described in Figure 1, using interwoven piano wires of diameter 0.3 mm, equidistantly spaced by 10 mm and supported by 9 actuators. First, the continuous mathematical model developed in previous studies will

be briefly recalled. Later, FEM computations will be considered.

### 3.1 Continuous mathematical model

A surface made from interwoven wires is of course a highly discontinuous function. However, one can show that reducing the wire spacing and diameter by the same factor will not change the maximum tension in the wire material and in the limit a continuous model is obtained. It was shown in [1] that under linear conditions the continuous surface shape is described by a fourth order partial differential equation with associated boundary conditions. The solution can be expressed by a combination of elementary solutions, one for each control point. The elementary solution is 1 at the position of the control point and 0 at the position of all the other control points. Once the elementary solutions are determined the total solution for arbitrary control point positions can be found extremely fast, a property which is very important inside an optimisation procedure.

It is worthwhile to notice that the equations defining the surface shape are the same for both the support net and the RF net introduced above. It is therefore, in principle, sufficient to attach the RF net to the support net at the control points. However, for reasons of manufacturing, testing and handling in general, it will be wise to use more attachments of the RF net across the surface, but this will not affect the surface shape.

### 3.2 FEM model

The main design driver from a mechanical point of view is that plastic deformations in the reconfiguration process of the antenna shall be avoided.

The basic mechanical properties of a woven net as function of the wire parameters are given in Table 1. The material data used in all FEM simulations can be seen in Table 2.

In the FEM calculations, the MSC MARC and NASTRAN software packages have been applied, MARC for the non – linear calculations and NASTRAN for the eigenfrequency determinations.

To simulate a woven net, a small model was set up. To keep the number of nodes and elements small, the FEM model wires are simulated as beam elements (1 dimensional element). A net of wires in X and Y direction is established, and all wires are located in the same XY plane. A contact radius is given as a property of the beams, implying that the MARC ‘beam to beam’ contact option can be used. The ends of the wires are constrained in all translations (See Figure 4).

In the first step of the weaving process, forces (~2.0 N, in opposite directions) are applied at all contact points to lift the wires free of each other (see Figure 4). These forces follow a ramp from zero up to full load (in this

process the wires can move freely through each other), and then they are ramped down to zero again. As the force is ramped down, the wires are touching and fall to rest on each other (See Figure 5). The last step is to release the constraints at the ends of the wires.

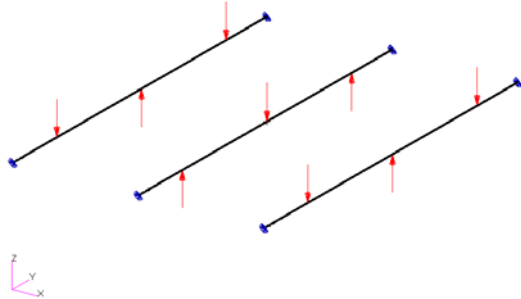


Figure 4 Forces and constraints applied to the Y-wires to bend them free of the X-wires (Not shown).

### 3.3 Approximate FEM model

The FEM woven model of Section 3.2 is very CPU consuming, because of the many elements and nodes necessary to describe the detailed curves of the wires. For models realistic in size (diameter e. g.  $\sim 1.5$  m) the FEM model has thus to be simplified. In order to do that, wires are simulated as beam elements. At the cross points between the wires, the nodes are connected to each other with rigid elements, which assure no translations.

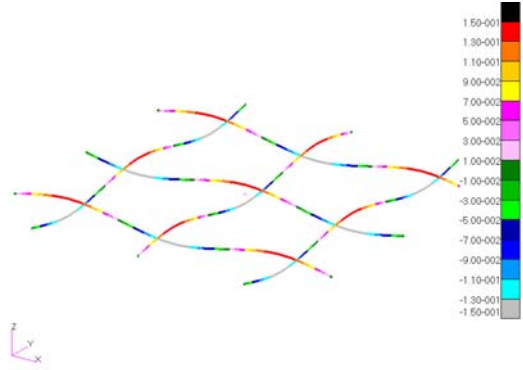


Figure 5 The Woven net. The legend shows deformations in Z-direction ( $\pm 0.150$  mm)

This approach was tried previously [6], but due to numerical problems their solution did not converge in the non-linear case.

The model still assumes piano wires with a diameter of 0.300 mm and the distance between the wires is 10 mm. This configuration has been chosen since the stresses are far from the Yield stress (Table 4). This leaves room for further bending of the net from the actuators, launch load etc.

The gain in size and computation time achieved by the approximate FEM model relative to the full FEM model of Section 3.2 for the prototype of Figure 1 can be seen in Table 3.

Table 1 Behaviour of the net as function of the wire parameters.

	Wire Stiffness	Contact Force	Bending Stress	Eigen frequency
Young's module E	E	E	E	$\sim E^3$
Yield stress	Unchanged	Unchanged	Unchanged	Unchanged
Diameter of wires D	$D^4$	$D^5$	$D^2$	$\sim D$
Distance between wires L	Unchanged	$L^{-3}$	$L^{-2}$	Decreases

Table 2 Material properties of piano wires.

Material Name			Piano wire
Young's module	E	MPa	210000
Poison's ratio	$\nu$		0.3
Shear module	G	MPa	80800
Density	$\rho$	kg/m <sup>3</sup>	7850
Yield stress	$\sigma$	MPa	2000

Both linear and non-linear models of the TICRA Lab Model with the deformations shown in Figure 6 have been obtained. This configuration was taken from [6, Fig. 2-2]. The main difference are movements of the actuators in the net plan. At the edge these movements are up to  $\approx 6$  mm in the direction to the centre, giving differences in the deformations of  $\approx 2$  mm.

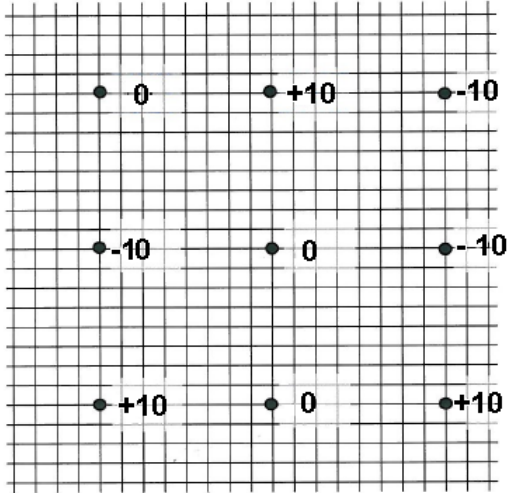


Figure 6 Displacements in mm added to both models in the 9 actuator points. Loads are taken from [6, Figure 2-2].

It is important that the fast, continuous model gives the sufficient accuracy. To check this it is compared with the FEM results. Figure 7 shows a comparison between the continuous model and the approximate, linear FEM model. It is seen that the agreement is better than 0.1 mm except in a few regions very close to the edge of the surface.

Figure 8 shows a comparison between the continuous model and the approximate, non-linear FEM model. The agreement is now less good with differences up to more than 1 mm. The reason to this is clearly the finite length of the wires and the associated displacement of the control points during the shaping of the surface. Ongoing investigations have indicated that it will be possible to include also this effect in the continuous model such that it can be used with confidence for realistic reconfigurable reflector designs.

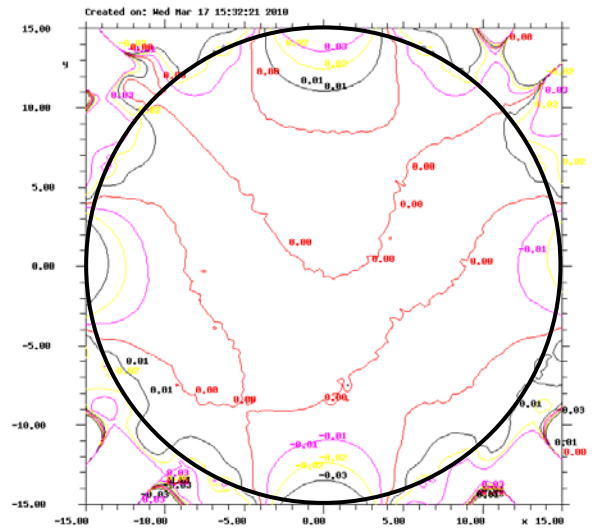


Figure 7 Differences between the continuous model and the approximate, linear FEM model. Dimensions in cm. Contour curves every 0.01 cm.

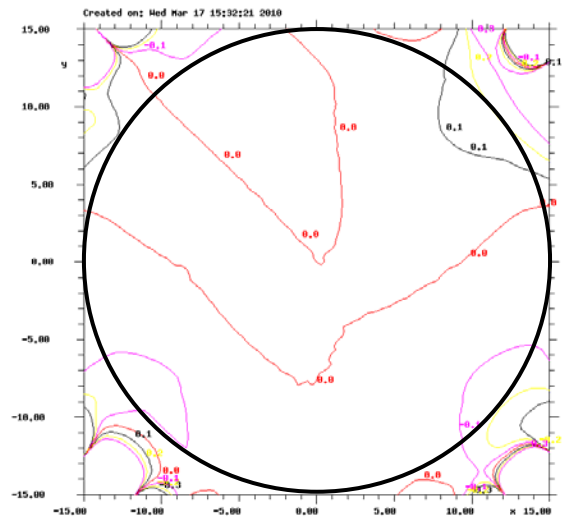


Figure 8 Differences between the continuous model and the approximate, non-linear FEM model. Dimensions in cm. Contour curves every 0.1 cm.

## 4 MECHANICAL PROPERTIES OF THE INTERWOVEN WIRE NET

### 4.1 The RF net

The thin RF net described in Section 2 is made by thin piano wires with a diameter of 0.030 mm. This diameter was chosen to avoid the problem with plastic deformations (Table 4). The bending stiffness of the wires changes as the diameter in fourth power, implying that the RF will simply follow the support net. Therefore, it is not necessary to take the stiffness of the RF net into account in the FEM model.

Although there are 10 times more thin than thick wires, their contribution to the total mass is only 1/10 of the support net

### 4.2 Eigenfrequencies for a full scale reflector

With the purpose to find the eigenfrequencies of a typical reflector of 1.5 m in diameter, an approximate FEM model, according to Section 3.3, was set up. The model gave rise to 53065 nodes and 70360 elements. The net is supported by 65 actuators. As expected, the eigenfrequencies are low. The first occurred at 12.8 Hz. The eigenfrequency where more than 10% of the mass of the reflector takes part in the movements, occurs at 16.4 Hz (See Figure 9). The total mass of this

reflector is only 225 grams. Therefore these low eigenmodes will have no impact on the rest of the satellite.

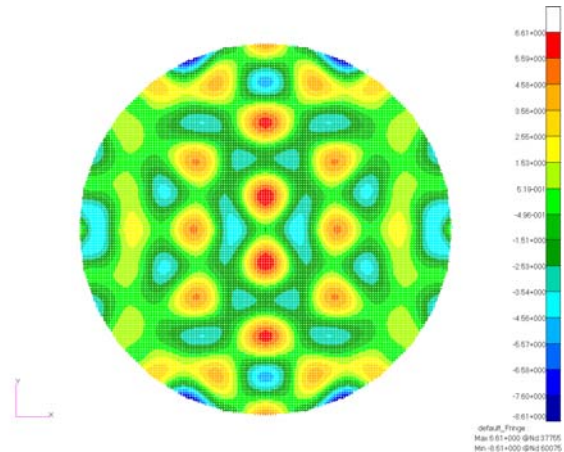


Figure 9 Eigen frequency pattern for the 1.5 m reflector supported by 65 actuators. The pattern shown is for 16.4 Hz which is the first eigenfrequency where more than 10% of the reflector mass takes part. The reflector mass is only 225 g.

Table 3 Model sizes and CPU time.

	Node	Elements	CPU-unit	CPU-time
Approximate model	15282	15220	Intel Duo CPU 6600 2.4 GHz	80 sec
Woven model	15282	15220	Intel Duo CPU P8400 2.26 GHz	6200 sec

Table 4 Bending stresses in wires of the net coming from weaving. A safety factor of 3.5 leaves room for further stresses coming from bending of the net with the actuators, launch loads and etc.

Wire Diameter	Distance Between wires	Young's module	Displacement	Area moment of inertia	Bending stress	Yield stress	Safety Factor
D mm	l/2 mm	E MPa	$u_{max}$ mm	I Mm <sup>4</sup>	$\Sigma$ MPa	$\Sigma$ MPa	
0.300	10	210000	0.300	$398 \cdot 10^{-6}$	567,5	2000	3.5
0.030	1	210000	0.030	$39.8 \cdot 10^{-9}$	567,5	2000	3.5

### 4.3 Reproducibility of the deformations.

To finally establish how well such an antenna can be deformed, we have investigated the deformations to an ideal paraboloid (diameter 1.8 m) based on deformation example shown in Figure 10. The model has 69 actuators placed 180 mm apart, with 104154 nodes and 103792 elements. Since we are only interested in calculating, how well we can reproduce the desired deformations, we have assumed that the paraboloid itself is established without any errors. The difference between the continuous model and the result obtained with the approximate, linear FEM model is given in Figure 11. It is seen that except close to the edge, the deviations are less than 50  $\mu\text{m}$ .

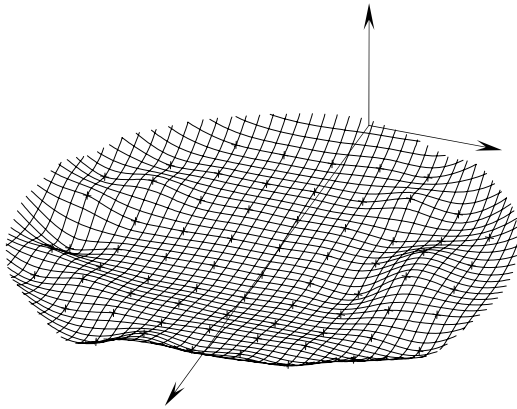


Figure 10 Shaping relative to parent paraboloid and magnified by 10. The 69 control points are shown by crosses and the surface shape is predicted by the continuous model.

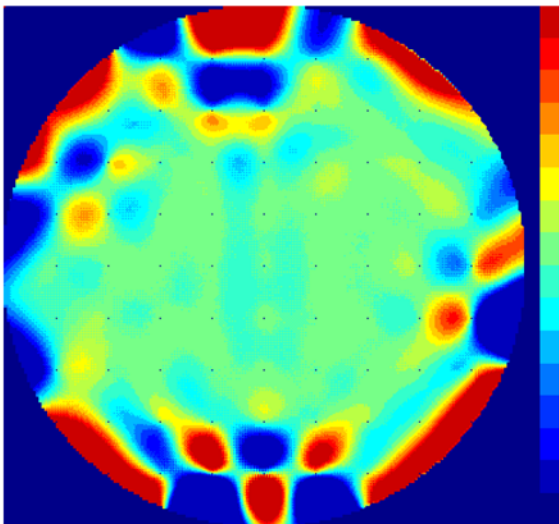


Figure 11 Differences between the continuous model and the approximate, linear FEM model (colour scale  $\pm 0.075$  mm).

### 4.4 Actuator connection

To shape the proposed reconfigurable reflector, actuators are needed. All actuators have a rod connected to a cross point in the support net (See Figure 13).

Simulations have shown that in order to be able to control the deformations of the net, the centre actuator needs to be constrained to only moving up and down, and two actuators on each of the wires going through the centre need to be constrained to only move in the radial direction. The design of the actuators assures that they can move freely with the net (See Figure 3 and Figure 12).

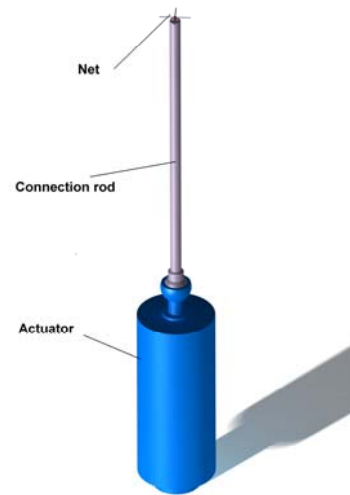


Figure 12 Actuator shown with connection rod to support net.

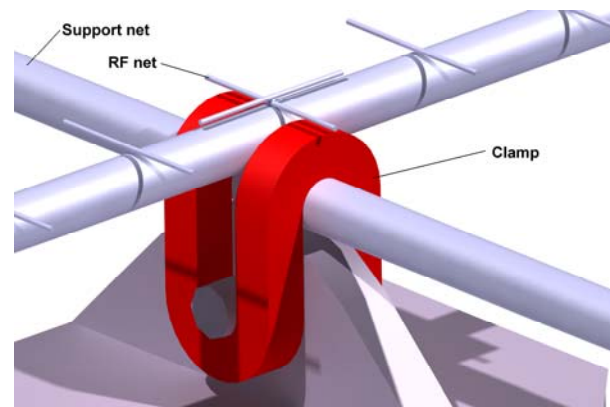


Figure 13 Detail of connection between rod from actuator and Support net.

## 5 CONCLUSIONS

An improved reconfigurable reflector technology able to provide reflectivity and reconfigurability at Ku-band was proposed. It was shown that the use of two nets, a coarse one supporting a fine one, controlled by a finite

number of control points can provide the necessary rigidity to be handled on ground and at the same time the necessary reflectivity and elasticity. Requirements on the degree of freedom of the control points were given.

It was later shown that the fine net can be neglected in the computation of the surface shape, due to its extremely light weight and low stiffness. A linear FEM analysis of the interwoven coarse net provided surface shape results in very good agreement with one given by the fast mathematical model developed in the past. Non-linear FEM analysis finally highlighted the importance of considering the non-linear behaviour of the net when shaping the antenna surface for a desired coverage on the Earth.

## 6 REFERENCES

- [1] Pontoppidan, K., "Light-weight reconfigurable reflector antenna dish", 28th ESA Antenna Workshop, Noordwijk, Holland, May 31–June 3, 2005
- [2] Baier, H.; Datashvili, L.; Langer, H.; Santiago-Prowald, J., "Shape Adaption and Mechanical Reconfiguration of Reflecting Surfaces", 29th ESA Antenna Workshop on Multiple Beams and Reconfigurable Antennas, 18-20 April 2007, ESA/ESTEC, Noordwijk, The Netherlands.
- [3] Pontoppidan, K.; Viskum, H.H., "Dynamic Link Improvements Using a Reconfigurable Reflector Antenna", 29th ESA Antenna Workshop on Multiple Beams and Reconfigurable Antennas, 18-20 April 2007, ESA/ESTEC, Noordwijk, The Netherlands.
- [4] Cappellin, C., Pontoppidan, K., "Feasibility Study and Sensitivity Analysis for a Reconfigurable Dual Reflector Antenna", EuCAP2009, 23-27 March 2009, Berlin, Germany.
- [5] Astrakhan, H.I. , "Reflecting and screening properties of plane wire grids", Radio Engineering, Vol. 23, No. 1, pp. 76-83, 1968.
- [6] Datashvili, L., "Orthogonal Wire Grid Modeling and FEM Investigations (Reconfigurable reflector concept by TICRA)", Technical Note TN-LLB-Recora-LD-014, 24 July 2008.
- [7] Cunningham, J.M., "A literature review to identify parameters influencing friction and wear data in space tribometer tests", ESA/TM/137, September 1993.